REPORT DOCUMENTATION PAGE

Form Approved
OMB No. 0704-0188

PLEASE DO NOT RETURN YOUR FORM TO THE ABOVE ORGANIZATION.

1. REPORT DATE *(DD-MM-YYYY)*	2. REPORT TYPE	3. DATES COVERED *(From - To)*
1 May 2006	Final Technical Report	1 May 2006-30 Apr 2007

4. TITLE AND SUBTITLE
Tribometer for Ultra Harsh Environments

5a. CONTRACT NUMBER
FA9550-06-1-0330

5b. GRANT NUMBER

5c. PROGRAM ELEMENT NUMBER

6. AUTHOR(S)
Dr. Ali Sayir

5d. PROJECT NUMBER

5e. TASK NUMBER

5f. WORK UNIT NUMBER

7. PERFORMING ORGANIZATION NAME(S) AND ADDRESS(ES)
Case Western Reserve University
Materials and Science
Cleveland, Ohio

8. PERFORMING ORGANIZATION REPORT NUMBER

9. SPONSORING/MONITORING AGENCY NAME(S) AND ADDRESS(ES)
USAF/AFRL
AFOSR
875 North Randolph Street
Arlington VA 22203

10. SPONSOR/MONITOR'S ACRONYM(S)

11. SPONSOR/MONITOR'S REPORT NUMBER(S)
AFRL-AFOSR-VA-TR-2016-0613

12. DISTRIBUTION/AVAILABILITY STATEMENT
Distribution Statement A: Approved for public release. Distribution is unlimited.

13. SUPPLEMENTARY NOTES

14. ABSTRACT
High temperature structural materials that exhibit structural, functional and multifunctional properties are needed to improve the performance of aeronautics and aerospace components. The major challenge for the application of materials at ultra harsh environments is the lack of understanding about their potential which is partly due to lack of experimental data at the harsh environmental conditions. In this report, we summarize the technical accomplishments for the Defense University Research Instrumentation Project (DURIP) that aims to develop a tribological test system for ultra–harsh environments

15. SUBJECT TERMS

16. SECURITY CLASSIFICATION OF:			17. LIMITATION OF ABSTRACT	18. NUMBER OF PAGES	19a. NAME OF RESPONSIBLE PERSON
a. REPORT	b. ABSTRACT	c. THIS PAGE			19b. TELEPHONE NUMBER *(Include area code)*

DEFENSE UNIVERSITY RESEARCH INSTRUMENTATION REPORT

Tribometer for Ultra – Harsh Environments

Submitted to:

AIR FORCE OFFICE OF SCIENTIFIC RESEARCH

Attention: **Dr. JOAN FULLER**

Non-Metallic Materials Program Manager

Attention:

PIE / DURIP

FA9550-06-1-0330

Point of Contact: **Dr. JOAN FULLER**

875 North Randolph Street,

Suite 325, 3112

Arlington, VA 22203

By

Dr. Ali Sayir

Research Associate Professor

Case Western Reserve University

Tribometer for Harsh Environments

SUMMARY

High temperature structural materials that exhibit structural, functional and multifunctional properties are needed to improve the performance of aeronautics and aerospace components. The major challenge for the application of materials at ultra harsh environments is the lack of understanding about their potential which is partly due to lack of experimental data at the harsh environmental conditions. In this report, we summarize the technical accomplishments for the Defense University Research Instrumentation Project (DURIP) that aims to develop a tribological test system for ultra–harsh environments.

The tribological test system (SRV 4) has been purchased from Optimol Corporation and has been modified to evaluate friction and wear characteristics of bulk materials and coatings. The tribological test system operate from -196°C to 1100 °C, in vacuum. The system is capable of analyzing material systems in oscillating-, rotating- and inclined angle combinations at frequencies up to 500 Hz at different lubricant configurations with viscosities ranging ten order of magnitude (solid-solid to solid-liquid). The tribological test system is able to measure tribological and physical properties at such diverse conditions spanning 10^{-8} Pa to ambient, and liquid nitrogen to high temperature. In addition to the development of tribological test system, we also purchased PVD75 film deposition system (Kurt Lesker Company) and we engineered the RF magnetron sputtering system so that it is able to deposit metallic-, semiconducting-, ionic- and coherently-bonded material systems for high temperature contact resistance and wide range other aeronautics and aerospace applications. The main thrust of the DURIP research project was focused on structural and multifunctional materials, specifically emerging materials for high temperature aerospace applications. We used directionally solidified oxide eutectic systems to demonstrate the capabilities of the tribological test system given that we have significant expertise on the eutectic and polyphase structured material systems. We used wide range of silicide systems to demonstrate the capabilities of RF magnetron sputtering film deposition system in view of the fact that silicides can have wide range of band gaps; from metallic (CrSi), semiconducting ($CrSi_2$) and semimetal (WSi_2).

The technical demonstration of the capabilities of both high temperature tribometer and film deposition system are complete and hence can provide a pathway for the collaboration of several universities, government laboratories and industry to evaluate next generation of aerospace materials. Currently, several international communities have been participating to investigate their materials using tribological test system at harsh environments.

I. INTRODUCTION

Case Western Reserve University (CWRU) engineered high temperature tribometer to test wear and friction characteristics of materials at high temperatures and ultra –harsh environments. The ultra-harsh environments are defined as temperatures ranging from -196 up to 1600 °C, and pressures ranging from atmospheric ambient pressure to ultra-high vacuum of 10^{-6} Pa. The project succeeded to meet all the requirements for vacuum, load (pressure), frequency, inclided loading configuration, environmental condition and temperature ranges from -196 °C to 1100 °C.

The most important (harsh) condition from the wear perspective for the aerospace materials was defined as the exposure to vacuum and ultra-high vacuum during excess to space. The liquid lubricants will not work in vacuum and only very few solids (with specific composition and structures) could be used in vacuum justify their use in the vacuum environment as harsh condition. Thus, our primary focus was on the design, engineering and testing of tribometer in high vacuum and high temperatures for the wear characteristics of materials. Loading configurations were ranging from the micro Newton to several kilo Newtons and frequencies up to 500 Hz. The two-year effort resulted in the development of tribometer with temperature capability exceeding 1100 °C (an increase of 900 °C from the current state-of-the-art) along with the associated development of the data analysis. The tribometer was design, built in a way to validate sliding, slip-rolling and rolling operations. We expect that capability of this tribometer for ultra-harsh environment will enable engineering designers and materials designers to interact. This interaction can provide platform (1) to leverage expertise and knowledge to reduce the time to develop, standardize, and implement high temperature structural and functional materials that can withstand ultra –harsh environments and (2) use tribological information to create strategies that link models at various length and time scales and provide bridge for the material specific information technologies.

II. MATERIALS SELECTION FOR WEAR TEST

Several mechanical properties of advanced ceramics make them suitable for tribological applications. Ceramics are being considered for very specific tribological applications that capitalize on a unique set of properties, Table 1. These properties are high hardness and compressive strength, retention of mechanical properties at elevated temperatures, resistance to chemical reactions, low density, high stiffness, and good electromagnetic characteristics. The applications described in Table 1 clearly show that ceramics are the enabling materials for

aeronautics applications and strongly relevant to Air Force's missions. There are additional challenges for aerospace applications necessitating new materials that will be used in severe space environment.* The increasing potential for the use of ceramics as components in lubrication systems has focused the attention to a better understanding their physical and chemical properties which will effect their behavior when in contact with themselves, other ceramics, or metals.

	Applications	Ceramics
Abrasion and erosion	Rocket nozzles Turbine blades in jet engines and steam turbine generators	SiC, CrC, WC SiC, SiALON
Corrosive Wear	Flow control operation, check valves Diesel injector needle valves and seals Space shuttle main engine	SiC, Al_2O_3, PSZ Si_3N_4,
High Temperature	High temperature bearings Valves, valve seats, cam followers Thrust-, journal-, ball- and roller bearings	Si_3N_4, PSZ, Al_2O_3/B_4C Al_2O_3/TiC, TiB_2
Low Density	Main bearing for turbines, ultra-high speed operations (100,000 rpm), high thrust and radial loads reaching 1000 °C, Seals, bushings	Si_3N_4, ceramic/steel racers
Electromagnetic	Cylinder liner in low heat rejection	Si_3N_4, Al_2O_3

Table 1 Current tribological applications of ceramics [6, 7, 8].

Ceramics, for the most part, do not have inherently good tribological properties. Friction coefficients in excess of 0.7 have been reported for example for silicon nitride sliding on itself or on bearing steel [6]. High friction at steady-state is accompanied by considerable wear. The upper temperature limit for the application of Si_3N_4 and Al_2O_3 are mainly limited from the reaction characteristics of bulk and/or surfaces to the tribological environment [7]. Si_3N_4 were shown to produce a thin silicon dioxide film with easy shear capability and to achieve low friction and low wear in a moist environment [8]. Al_2O_3 ceramics were also found to produce soft

* In the United States alone a large number of spacecraft failures. More demanding requirements have been causing failures to occur during the qualification testing of future satellites and space platform mechanism even before they are launched (e.g. GOES-NEXT, CERES, Space station beta joints etc.) [5]

aluminum hydroxide film on their sliding interfaces and display low friction when tested in water. The removal of the lubricant at elevated temperatures causes friction coefficient increases with associated poor wear performance. Despite the inherently poor tribological properties, Si_3N_4 and Al_2O_3 ceramics were successfully applied because of their improved strength and toughness [7, 8]. The significant amount of possibilities exists for non metallic materials with low friction coefficients.

When a ceramic is brought into contact with another ceramic, or metal, strong bond forces can develop between the materials. The bonding forces will depend upon the state of the surface, cleanliness, and fundamental properties of the two solids, both surface and bulk. Elastic, plastic, and fracture behavior of ceramics in solid-state contact are related to friction and wear. Conventional ceramics fail with transgranular localized fracture under contact loads. It appears that for these materials to have a significant application possibilities in future tribo-systems, new means must be developed to reduce their friction and wear. Specifically, ways must be found to prevent localized fracture.

The proposed program advocates directionally solidified eutectic ceramics for applications involving severe tribological (e.g., high temperature, corrosive media, vacuum environment, high load and speed). The eutectic architecture, a continuous reinforcing phase within a higher volume phase or matrix, can be described as a naturally occurring *in-situ* composite. *In-situ* composites exhibit mechanical properties intermediate between monolithic materials and man-made composites. The directionally solidified eutectic samples 2 – 4 mm in diameter have been evaluated using NASA Glenn Research Center high-temperature, unidirectional-sliding, wear apparatus. The wear rate of the directionally solidified eutectic were in the range of $1.8x10^{-10}$ $mm^3/N•m$ to $3x10^{-8}$ $mm^3/N•m$ and the coefficient of friction 0.4. These are excellent results. The wear rates at the order of 10^{-6} $mm^3/ N•m$ or less are considered to be very good (wear criteria [6, 7, 8]). The wear rate of eutectic is four-orders of magnitude lower than so called 'very good wear resistance' materials and further optimization of composition, phase

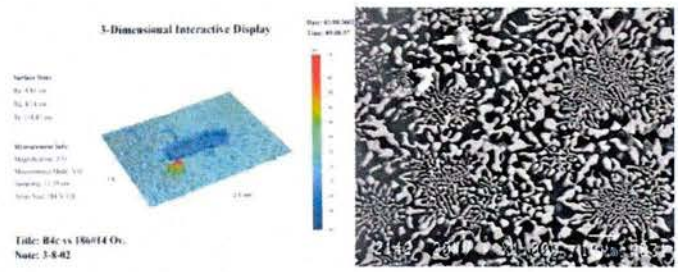

Fig. 1 Wear tracks of directionally solidified $Al_2O_3/ZrO_2(Y_2O_3)$ eutectic ceramic and B_4C.

content and processing parameters reduced the wear even further as will be described next section (Fig. 2).

Y_2O_3	Ta_2O5	TiO_2
6	5	8

Table 2 Constituent elements (excluding ZrO_2+Al_2O_3) [mol %]

The wear properties of two-phase eutectic are superior to that of the constituent alone due to strong constraining effects provided by the interlocking microstructure of directionally solidified eutectics. The large aspect ratio and strong interphase bonding (almost coherent [9, 10]) found in directionally solidified eutectics contributes to their superior wear resistance, compared to that of conventional ceramics. Thus, localized fracture under the normal and tangential forces are reduced dramatically and wear resistance increased. The phases comprising a eutectic are thermodynamically compatible at higher homologous temperatures than man-made composites and as such offer the potential for superior high temperature properties. Hence, high temperature wear properties of directionally solidified eutectics are also expected to be superior to conventional ceramics. This brief summary demonstrates that directionally solidified eutectic ceramics have much to offer for future tribological applications.

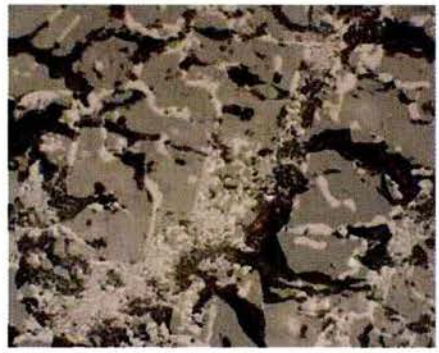

Fig. 2 SEM micrograph of specimen surface

In this DURIP project, we focused on the testing a directionally solidified $Al_2O_3/ZrO_2(Y_2O_3/TiO_2)/Ta_2O_5$ system to demonstrate the capabilities of the tribometer. The $Al_2O_3/ZrO_2(Y_2O_3/TiO_2)/Ta_2O_5$ system is a $Al_2O_3/ZrO_2(Y_2O_3)$ eutectic with TiO_2 and Ta_2O_5 additions. The TiO_2 and Ta_2O_5 additions easily reduces during solidification in argon and therefore provide $Al_2O_3/ZrO_2(Y_2O_3)$ eutectic with Ti and Ta metal additions. The heterogeneous structure of this cermet (oxide and metal) provide unique opportunity and challenges and thus was selected as a material to test the tribometer. The constituent elements are shown in Table 2. The Young's modulus was measured to be 330 GPa. Figure 2 shows a scanning electron microscope (SEM) micrograph of the ceramic. It was seen that the developed poly-phase eutectic ceramic is heterogeneous and exhibits distinct $Al_2O_3/ZrO_2(Y_2O_3)$ eutectic phase and metal phases. Figure 3 shows x-ray diffraction (XRD) of the ceramic produced by energy dispersive spectroscopy. Although the existence of the metal phases was observed in Fig. 1, there were no metal phases, Ta_2O_5 or TiO_2, detected in x-ray analysis (Fig. 3) indicating

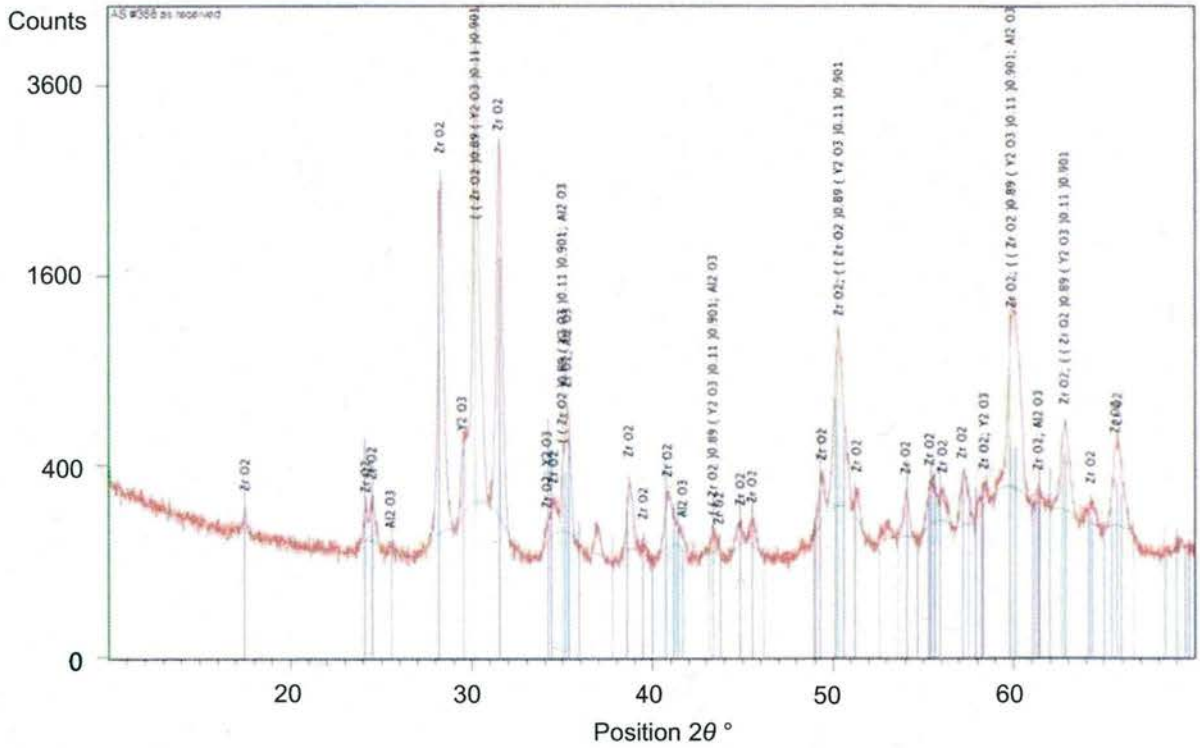

Fig. 3 X-ray diffraction of specimen

that the volume fraction of the metallic phase is below the detection limit of x-ray.

Figure 4 shows the three-dimensional shape of the specimen surface measured by an optical profiler. The surface roughness was 63.3 μm *Rz* and 1.04 μm *Ra*, and, the specimen has many pits on the surface, which resulted in the high *Rz* value. The area excluding the deep pits was measured around 30-40 μm *Rz* and 0.6-0.8 μm *Ra*. The heterogeneous poly-phases resulted in the unevenness of the specimen surface.

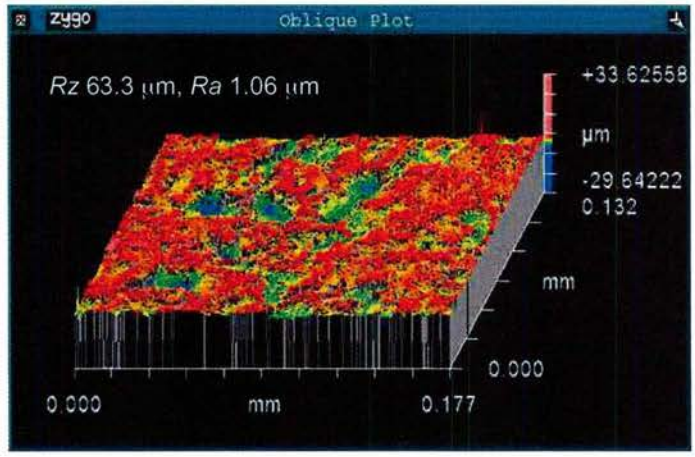

Fig. 4 Three-D shape surface measured by optical profiler

III. TRIBOMETER DESIGN AND TEST

Figure 5 shows a schematic of the sliding tests. Reciprocating sliding friction experiments, called sliding tests, were conducted with a 10 mm diameter $ZrO_2(Y_2O_3)$ ball on the eutectic ceramic to understand the wear and friction properties using the SRV-4 friction and wear tester (Optimol Instruments, Germany). The specimen (4×12×1.4 mm) was rinsed with ethanol using an ultrasonic cleaner and was mounted into the stainless steel holder, which was set on the temperature-controllable stage. The temperature ranges from -70 to 900 °C. The ball was also rinsed with ethanol and mounted in the holder. It was pressed against the specimen surface with a normal force *F*n in the range from 1 to 2000 N from above and was oscillated in the horizontal direction with pre-set amplitude and frequency. The minimum reading load of the equipment was 1 N. The maximum frequency was 511 Hz, and the maximum stroke was 5 mm. In case of the 5 mm stroke, the frequency must be limited to around 50 Hz. The friction force *Ft* was detected, and the coefficient of friction *Ft*/*F*n was calculated.

Figure 5 (a) shows an external view of the testing equipment, and Fig. 5 (b) shows the interior of the chamber. The sliding test unit is set inside the chamber. The chamber can be rotated in the counterclockwise direction; this enables the sliding direction of the ball to be controlled from the horizontal to the vertical direction. The pressure inside the chamber can be changed from ambient to vacuum conditions. The temperature of the stage inside the chamber can be heated or cooled by means of the chiller connected to the stage.

Table 3 shows conditions of oscillating sliding friction experiments. The ball was oscillated with a 1000 μm stroke at 20 Hz. The mean sliding speed was calculated to be 0.04 m/s. The load *F*n was changed in the range of 2-10 N. The sliding tests were performed with dry conditions at 25-300 °C for 1 hr, 72000 cycles, and the coefficients of friction *Ft*/*F*n were recorded. After the sliding tests, the specimen was cleaned for 20 min with ethanol in an ultrasonic cleaner, and the scratches generated by the sliding tests were observed by microscopy. It is noted that the experiments were repeated at least three times in each condition and the data shown in this report demonstrate representative trends.

III.1 Effects of the Environment and Temperature on Wear Properties

Initially, the effects of the stage temperature on the *Ft/Fn* were examined at 25-300 °C. Figure 7 shows the changes in *Ft/Fn* with the ball reciprocating cycle. As shown in Fig. 3, the value *Ft/Fn* and its deviation were smallest in the case of 25 °C. The friction heat was generated at the contact area of the ball against the specimen. This must cause the reduced metal phases, generating pits. The uneven surface led to the severe sliding conditions between the ball and specimen surfaces, increasing the wear rate of the ball. The wear debris trapped between the ball and specimen increased the value of *Ft/Fn*. Since the wear debris are free grains, they can be trapped in the sliding area and pushed away from the area due to the sliding motion of the ball. This resulted in the irregular deep scratches on the specimen surface, as shown in Fig. 8 (indicated by red circles). The deep scratches were clearly observed in the cases at 50 °C and 100 °C shown in Figs. 8 (b) and (c). In the case of 100 °C (Fig. 8 (c)), the deep scratches became wider than those of Fig. 8 (b), which is due to the larger amount of the debris trapped between the ball and specimen surfaces. Figure 8 (d) shows the 300 °C case , in which the scratches are barely observed. Instead, the specimen surface was covered by the wear debris regardless of the careful rinsing by the ultrasonic cleaner. Increased amounts of wear debris resulted in the deterioration of the deviation of *Ft/Fn* as illustrated in Fig. 6.

The sliding area of the specimen was further observed by microscope with a high magnification. Figure 9 shows a representative micrograph of the surface after testing at 50 °C; it is a high magnification section of Fig. 8 (b). The $Al_2O_3/ZrO_2(Y_2O_3)$ eutectic phase was clearly observed, and the haze around the eutectic phases was residue of the wear debris (even though the specimen was rinsed after the sliding tests). This proved the appearance of the wear debris between the ball and specimen surfaces, which increase the *Ft/Fn* value.

According to the results summarized in Fig. 7, the *Ft/Fn* ratio was initially irregular but stabilized after 54000 cycles. Therefore, the values of the *Ft/Fn* ratio in such stabilized conditions are discussed. Figure 10 shows the relationship between *Ft/Fn* and temperature of the stage after 60000 cycles. The *Ft/Fn* value and standard deviation were 0.56 and 0.013 at 25 °C, 1.14 and 0.055 at 50 °C, 0.94 and 0.055 at 100 °C, and 1.00 and 0.034 at 25 °C, respectively. It is seen that the conditions with the lowest temperature of the four, 25 °C, showed the smallest standard deviation.

An important condition affecting the debris behavior that was observed during the sliding tests. The experimental setup used for this research, SRV-4 wear and friction tester,

automatically controls the load *F*n during the tests. For example, the load *F*n was reduced to maintain the set load if the specimen holder expanded and pushed the specimen from the bottom to the ball. Here, the resolution was 1 N, which is 10 % of the load applied in the experiments. The load reduction generally causes a slight clearance between the ball and specimen surface. This increased the potential for wear debris to be trapped in the clearance between the ball and specimen surfaces. In turn, the *Ft*/*F*n value was irregular. This phenomenon was seen more often at higher temperatures. As described above, the presence of wear debris causes the standard deviation to deteriorate.

The sliding tests were performed for 72000 cycles at each of the temperatures (25, 50, and 100 °C), for a total of 216000 cycles for the experiment. Figure 11 shows the experimental results. The irregular drops in *Ft*/*F*n due to the load control system of the setup were clearly observed, and the frequency of occurrences increased at 100 °C. Excluding these dropped values, the standard deviation became less than 0.01 regardless of the set temperature. The *Ft*/*F*n values at 25, 50, and 100 °C are 0.5, 0.6, and 0.7, respectively. While *Ft*/*F*n at 25 °C showed a value similar to Fig. 6, the other conditions showed smaller values than the cases in Fig. 7. The milder conditions resulting from gradually increasing the temperature of the stage must discourage the debris trapped in the clearance between the ball and specimen surfaces. Comparing Fig. 12 with Fig. 8 (c), the irregular deep scratches in Fig. 12 were less than those in Fig. 8. However, the trends in *Ft*/*F*n with temperature were similar to the previous experiments.

Accordingly, these tests demonstrated that the high-temperature atmosphere encourages the reduced the metal phases, creating pits on the specimen. The specimen surface scratched the ball surface and generates wear debris. The debris trapped between the ball and specimen surfaces encourages abrasion as well as the increase of the value of *Ft*/*F*n.

It is important to perform the sliding tests excluding the effects of the wear debris on *Ft*/*F*n to understand the material properties of the developed ceramics. The experimental conditions are changed from severe to mild by reducing the load on the ball. Next, the sliding tests were performed with various loads reduced to 2-8 N at the set temperature of 25 °C. The other conditions followed Table 3.

Figure 13 shows relationship between *Ft*/*F*n and load *F*n at 25 °C at the 72000 cycles. The dark bar shows the conditions using the same specimen used in the previous tests. The minimum load reading, 1 N, represented 50 % of the load during the experiments in the 2 N case,

25 % with 4 N, 16.6 % with 6 N, and 12.5 % with 8 N. In particular, the load control system affected the instability of *Ft*/*Fn* in the 2 N and 4 N conditions. Except for these cases, *Ft*/*Fn* is considered about 0.5, similar to the previous results with 10 N. This must be intrinsic to this condition, and the experimental conditions must be reasonable for testing this ceramic.

III.2 Wear Properties at High-temperature

One of the important objectives is to find the tribological behavior of the ceramic at high-temperature environment, over 1000 °C. To investigate high temperature properties, the specimen was heat treated at 1200 °C for 1 hr and cooled down to room temperature in an air. Another specimen was prepared by heat treatment at 1600 °C. With these specimens, the sliding tests were performed at 25 °C following Table 3.

The results were added in Fig. 13. The heat-treated specimens showed similar trends in the conditions with 6-10 N, and the *Ft*/*Fn* values were higher than those of the non-heat-treated specimen. Figure 14 shows the surfaces after testing of the specimens heat-treated at 1200 °C and 1600 °C. The metal phases as well as the scratched mark are barely seen on the surface of the material heat-treated at 1600 °C. The high-temperature environment must encourage the oxidation of the metal phases, reducing the toughness and increasing the brittleness. This resulted in the high *Ft*/*Fn* values and decreased the wear resistance. Although the effects of the heat treatment temperature between 1200 °C and 1600 °C must be very small this time, more experiments are be required to determine the material properties of the ceramic in high-temperature environments.

The sliding experiments were also performed on $Al_2O_3/ZrO_2(Y_2O_3)$ eutectic ceramic without metallic phases, which was previously developed [1] to understand the effects of metal phases on the wear properties. The composition of the ceramic was ZrO_2 33.69 mol%, Y_2O_3 1.24 mol%, and Al_2O_3 65.07 mol% [1]. The sliding tests followed Table 2 with a 10 N load at 25 °C. Figure 15 shows the changes in *Ft*/*Fn* with cycle for the ceramic with and without metal phases. It is seen that the ceramic containing metal phases shows about a half *Ft*/*Fn* of the ceramic without metal phases. Figure 16 shows the micrograph of the specimen surface without metal phases after testing. Deep scratches generated by the debris trapped between the ball and specimen surfaces were observed. The lower toughness and higher brittleness must cause the deeper scratches than found in the ceramic containing metal phases. This demonstrates that adding metal phases into the ceramic must improve the wear resistance.

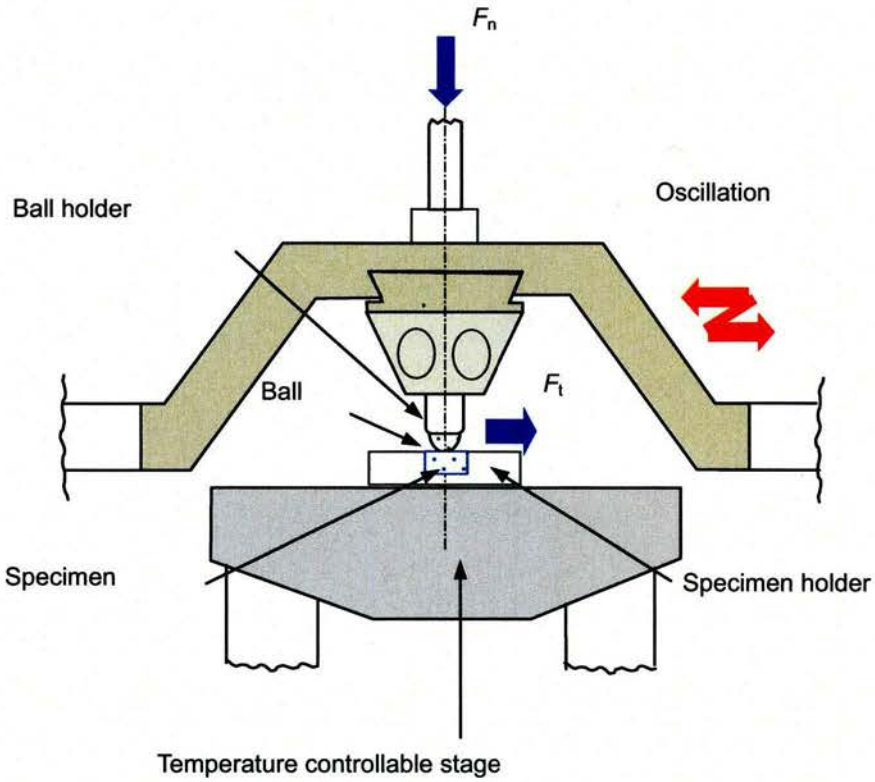

Fig. 5 Two-dimensional schematic of sliding tests

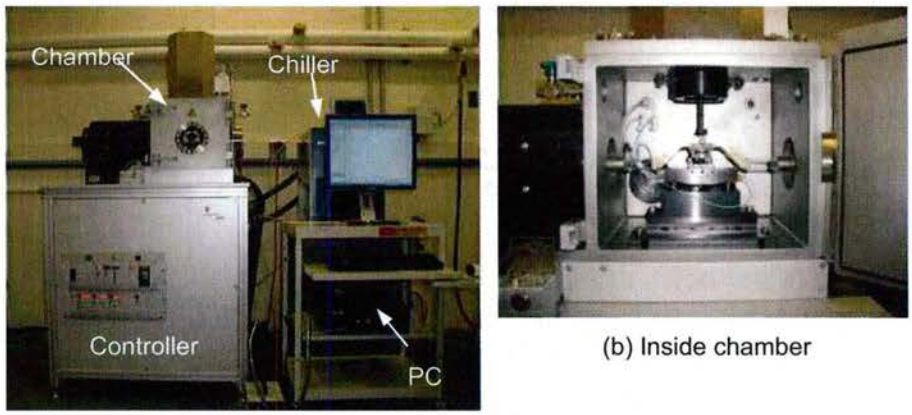

(a) External view of setup

(b) Inside chamber

Fig. 6 Photograph of experimental setup

Table 3 Conditions of reciprocating sliding friction experiments

Stroke	1000 μm
Frequency	20 Hz
Load	2-10 N
Number of cycles	72000
Mean sliding speed	0.04 m/s
Lubricant	None (dry)
Temperature	25-300 °C

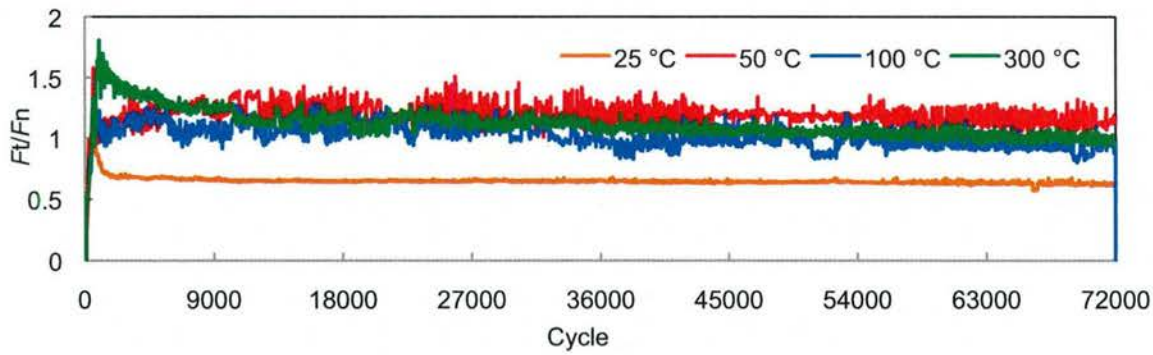

Fig. 7 Changes in *Ft*/*Fn* with cycle

(a) Temperature 25 °C (b) Temperature 50 °C

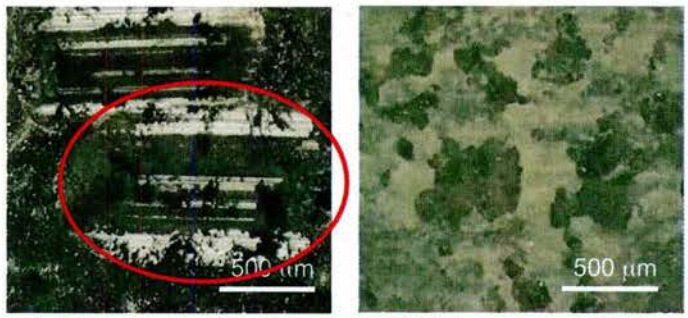

(c) Temperature 100 °C (d) Temperature 300 °C

Fig. 8 Micrographs of surfaces after testing for 72000 cycles

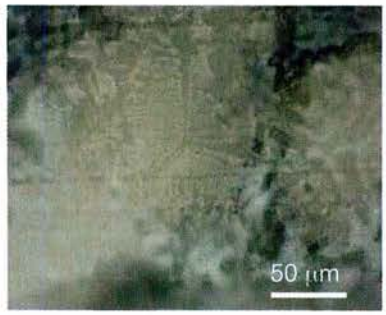

Fig. 9 Micrograph of surface after testing for 72000 cycles at 50 °C with high magnification

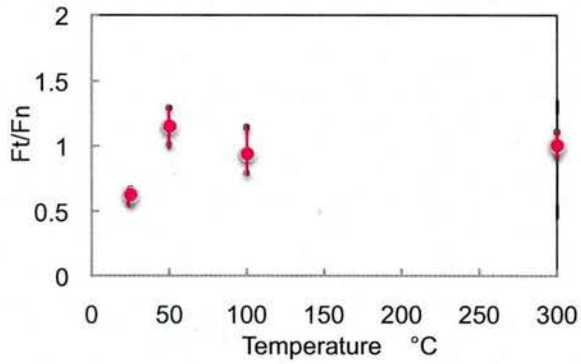

Fig. 10 Relationship between *Ft*/*Fn* and temperature after 60000 cycles

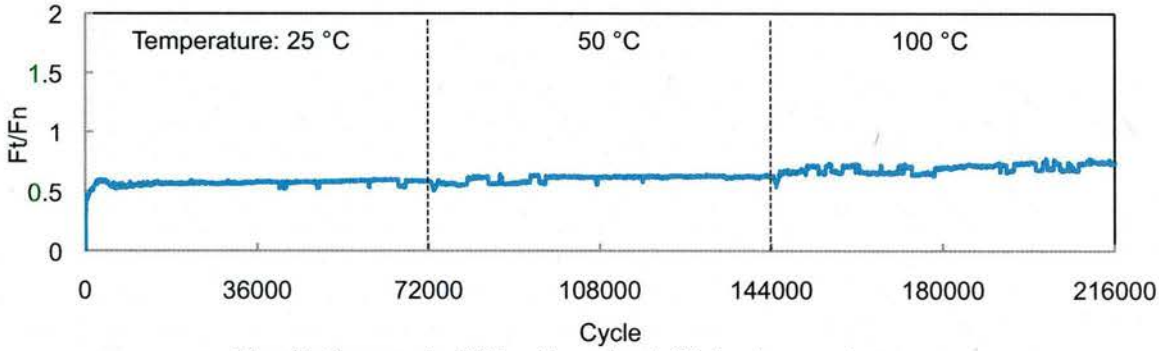

Fig. 11 Changes in *Ft*/*Fn* with cycle at differing temperatures (72000 cycles at each temperature: 25, 50, and 100 °C)

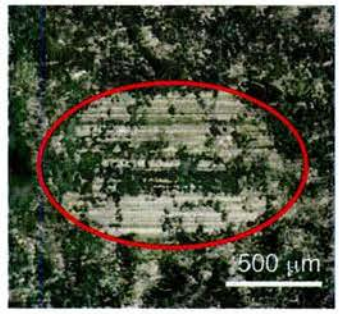

Fig. 12 Micrograph of surface after testing for 216000 cycles (Temperature was changed from 25 to 50 to 100 °C every 72000 cycles.)

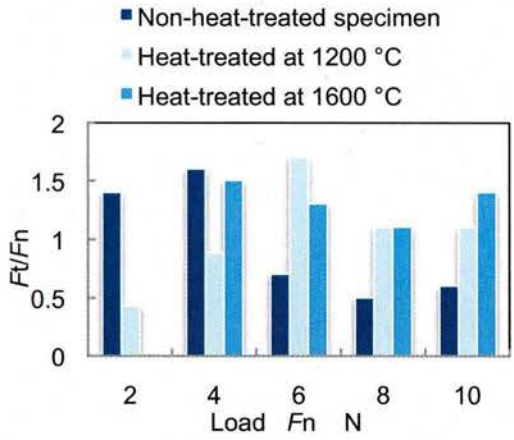

Fig. 13 Relationship between *Ft*/*Fn* and load *Fn* at 25 °C at 72000 cycles

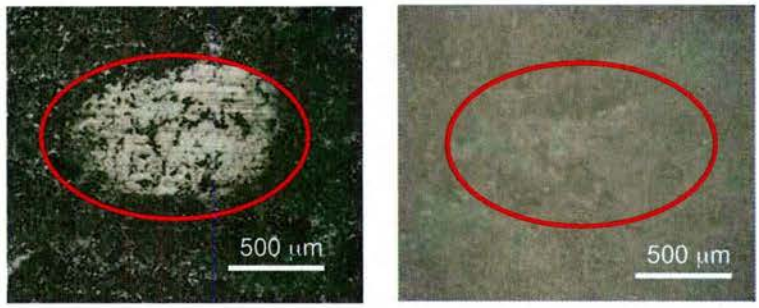

(a) Specimen heat-treated at 1200 °C (b) Specimen heat-treated at 1600 °C

Fig. 13 Micrograph of surfaces after testing with a load of 8 N at 25 °C for 72000 cycles

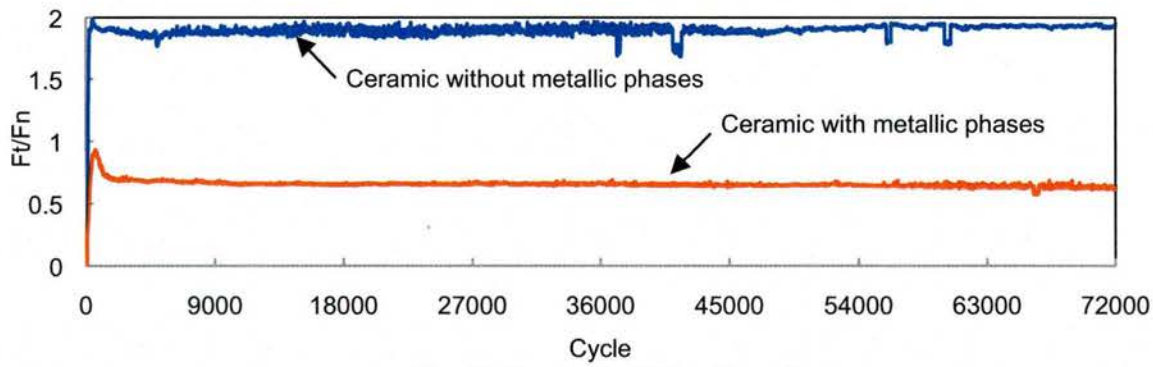

Fig. 15 Changes in *Ft*/*Fn* with cycle

Fig. 16 Micrograph of surface after testing of specimen without metal phases

IV. REFERENCES

1. F. Christin, "Design, Fabrication and Application of C/C, C/Si And SiC/SiC Composites," In: High temperature Ceramic matrix Composites, Eds.: W. Krenkel, R. Naslain, H. Schneider; WILEY-VCH, Weinheim, 2001, ISBN 3-527-30320-0.

2. M. Dogigli*, H. Weihs**, K. Wildenrotter*, H. Lange, "New High-Temperature Ceramic Bearing," 51st International Astronautical Congress, 2-6 OCT 2000, Rio De Janeiro, Brazil, PAPER IAF-00-I.3.04.

3. H. Pfeiffer and K. Peetz, "All-Ceramic Body Flap Qualified for Space Flight on the X-38," 53rd Int. Astronautical Congress, Houston, TX, USA, 10.-19. Oct. 2002. Int. Astronaut cal Federation, F-75015 Paris

4. K. Miyoshi, K. W. Street Jr., R. L. Vander Wal, R. Andrews and A. Sayir, "Solid Lubrication by Multiwalled Carbon Nanotubes in Air and in Vacuum," Tribology Letter, 19 [3] (2005) 191 – 201.

5. K. Miyoshi, "Aerospace Mechanisms and Tribology Technology: Case Study," in "Solid Lubrication Fundamentals and Applications," Marcel Dekker, Inc., New York (2001) pp. 293-332.

6. D. H. Buckley and K. Miyoshi, "Fundamental Tribological Properties of Ceramics, " Eng. Sci. Proc. [6] (1985) 9191-939.

7. H. E. Sliney, T. P. Jacobson, D. Deadmore, and K. Miyoshi, Tribology of Selected ceramics at Temperatures to 900 °C," Ceram. Eng. Sci. Proc. [7] (1986) 1039-11051.

8. K. Miyoshi, "Solid Lubrication Fundamentals and Applications," Marcel Dekker, Inc., New York (2001) pp.145-217.

9. A. Sayir and S. C. Farmer, "The Effect of the Microstructure on Mechanical Properties of Directionally Solidified $Al_2O_3/ZrO_2(Y_2O_3)$ Eutectic," Acta Mat., 48 (2000) 4691 - 4697.

10. C. Frazer, E. Dickey and A. Sayir, "Crystallographic Texture and Orientation Variants in $Al_2O_3/Y_3Al_5O_{12}$ Directionally Solidified Eutectic Crystals," J. Crystal Growth, 232 [1-2] (2001) 187- 195.

11. M. E. Campbell, "Solid lubricant – a survey," NASA SP-5059(01), 1972.

12. J. K. Lancaster, "Solid Lubricants," CRC Handbook of lubrication – theory and practice of tribology (E.R. Booser, ed.), CRC Press, Boca Raton, FL., vol. II, 1984, pp. 269 – 290.

13. S. Iijima , Helical microtubules of graphitic carbon. Nature 1991; 354 (6348)56 – 58.

14. M.-F. Yu, B.S. Files, S. Arepalli, and R.S. Ruoff, "Tensile Loading of Ropes of Single Wall Carbon Nanotubes and their Mechanical Properties" Phys. Rev. Lett., 84, (2000) 5552 - 5555.

15. L. JolyPottuz, F. Dassenov, B. Vacher, J.M. Martin, and T. Mieno, "Ultralow Friction and Wear Behaviour of Ni/Y-based Single wall Carbon Nanotubes," in "Novel carbons in tribology," eds. K. Miyoshi & K.W. Street, Tribology International, vol. 37, Special Issues 11–12, 2004, pp. 1013 - 1018.

16. A. Sayir, M. H. Berger, J. Fuller, and Y. Waku, eds. "Directionally Solidified Eutectic Ceramics," special issue of J. Europ. Ceram. Soc., 25 (2005) pp.1191 – 1462.

17. D. Tabor, "Status and Direction of Tribology as a Science in the 80's- Understanding and Prediction, New directions in Lubrication, Materials, Wear, and Surface Interactions,"W. R. Loomis, ed. Noyes Publications, Park Ridge, NJ Vol.1 1985.

18. K. Miyoshi, "Design, Development, and Its applications of Novel Techniques for Studying Surface Mechanical Properties, Interfaces Between Polymers, Metals, and Ceramics, Mat. Res. Soc., Vol. 153 (1989) 321 -330.